Nonlinear photonic crystal microdevices for optical integration

Marin Soljačić, Chiyan Luo, and J. D. Joannopoulos

Department of Physics, Massachusetts Institute of Technology, Cambridge, Massachusetts 02139

Shanhui Fan

Department of Electrical Engineering, Stanford University, Palo Alto, California 94304

Received October 14, 2002

A four-port nonlinear photonic crystal system is discussed that exhibits optical bistability with negligible backscattering to the inputs, making it particularly suitable for integration with other active devices on the same chip. Devices based on this system can be made to be small [$O(\lambda^3)$] in volume, have a nearly instantaneous response, and consume only a few milliwatts of power. Among many possible applications, we focus on an all-optical transistor and integrated optical isolation. © 2003 Optical Society of America

OCIS codes: 190.4360, 190.1450.

Photonic crystals (PCs) represent a promising platform for eventual large-scale integration of optical components and devices. To achieve active, high-speed functionality (including, e.g., wavelength conversion or all-optical switching), one must incorporate nonlinear materials into PCs. In this regard, exploration of nonlinear optical bistability in PC defect complexes is particularly attractive for the implementation of many all-optical operations.[1] The feasibility of observing bistability at telecommunication speeds, with only a few milliwatts of power, has already been proposed in a class of small [$O(\lambda^3)$] PC two-port devices.[2,3] In this Letter we describe a novel device system with four ports that provides very important new performance characteristics. For example, essentially no portion of the incoming pulse is ever reflected back into the input waveguide, which is of crucial importance for integration with other active devices on the same chip. Through the use of analytical theory, and detailed numerical simulations, we explain this device's underlying physics and demonstrate its operation as an all-optical transistor and for optical isolation.

Ideally, for many applications one would like to have a device with two inputs whose output has a strong dependence on the (weak) amplitude of one of its inputs (the probe input). Moreover, for ultimate efficiency, one would require single-mode waveguiding, high-Q cavities, and controllable radiation losses. A nonlinear PC system can provide us with all these capabilities.

The system that we propose, shown in Fig. 1, is reminiscent of the channel-drop filter introduced in Ref. 4. The critical difference is that in our system the PC is made from high-index nonlinear rods suspended in air, and this leads to important new functionality. The rods are made from an instantaneous Kerr material with an index change of $nc\epsilon_0 n_2|\mathbf{E}(x, y, t)|^2$, where n_2 is the Kerr coefficient. The system consists of two waveguides and two single-mode high-Q resonant cavities. The even and odd states supported by the two-cavity system are designed to be degenerate both in their resonant frequencies and in their decay times. Signals propagating rightward couple only to a particular superposition of the two states that in turn decays into only rightward-propagating signals; consequently, there is no reflection in the leftward direction. Since the energies stored in the two cavities are always equal, the presence of nonlinearity does not spoil the required left–right symmetry of the system.[5] Consequently, to the lowest order, the only influence of the nonlinearity is to change the doubly degenerate resonant frequency, ω_{RES}, depending on the intensity of the signal.

For a weak cw signal at ω, applied at port 1, the output at port 4 is given by $T_4(\omega) \equiv P_{\mathrm{OUT4}}(\omega)/P_{\mathrm{IN1}}(\omega) = \gamma^2/[\gamma^2 + (\omega - \omega_{\mathrm{RES}})^2]$, where P_{OUT4} and P_{IN1} are the outgoing and incoming powers, respectively, and γ is the width of the resonance; the output at port 2 is given by $T_2(\omega) = 1 - T_4(\omega)$, whereas the outputs at 1 and 3 are zero for all frequencies. Given these forms for the transmission, using

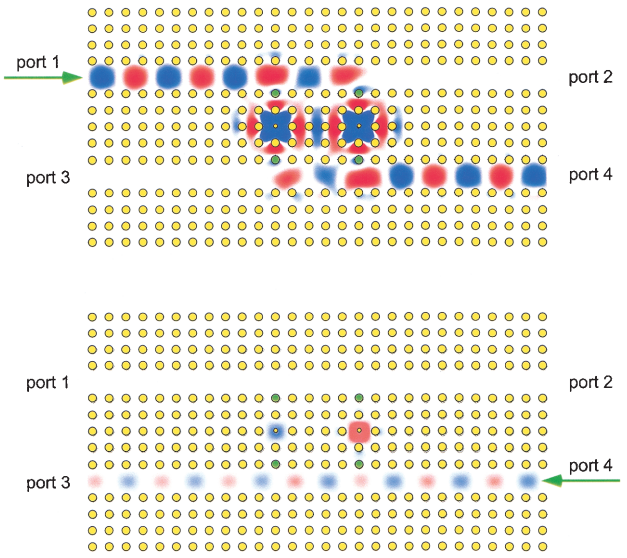

Fig. 1. Basic four-port nonlinear PC devices that we use to demonstrate optical bistability. The PC consists of high-index, $\epsilon_H = 11.56$, rods with radius $0.2a$; a is the lattice constant. The green rods have $\epsilon = 9.5$; the small rods have $\epsilon = 6.2$ and radius $0.05a$. As an example of the use of the device, we show the electrical fields when it performs optical isolation. Top, a strong forward-propagating pulse; bottom, a weak reflected backward-propagating pulse. We model the high-index rods as having an instantaneous Kerr nonlinearity.

0146-9592/03/080637-03$15.00/0

perturbation theory with a small nonlinear index change, one can self-consistently find the nonlinearly induced resonance shift, and thereby the steady-state transmission of cw signals through the system. Such analysis shows[2] that the system will exhibit optical bistability if the carrier frequency ω_0 is sufficiently below the resonant frequency, $\delta \equiv (\omega_{\mathrm{RES}} - \omega_0)/\gamma > \sqrt{3}$, and that the steady-state values of the cw powers are ${P_{\mathrm{OUT4}}}^S/{P_{\mathrm{IN1}}}^S = 1/[1 + ({P_{\mathrm{OUT4}}}^S/P_0 - \delta)^2]$, and ${P_{\mathrm{OUT2}}}^S/{P_{\mathrm{IN1}}}^S = 1 - {P_{\mathrm{OUT4}}}^S/{P_{\mathrm{IN1}}}^S$, where characteristic power $P_0 \equiv 1/[\kappa Q^2(\omega_{\mathrm{RES}}/c)n_2(\mathbf{r})|_{\mathrm{MAX}}]$ and κ is a measure of nonlinear feedback given by

$$\kappa \equiv \left(\frac{c}{\omega_{\mathrm{RES}}}\right)^d * \frac{\int_{\mathrm{VOL}} \mathrm{d}^d\mathbf{r}[|\mathbf{E}(\mathbf{r})\cdot\mathbf{E}(\mathbf{r})|^2 + 2|\mathbf{E}(\mathbf{r})\cdot\mathbf{E}^*(\mathbf{r})|^2]n^2(\mathbf{r})n_2(\mathbf{r})}{[\int_{\mathrm{VOL}} d^d\mathbf{r}|\mathbf{E}(\mathbf{r})|^2 n^2(\mathbf{r})]^2 n_2(\mathbf{r})|_{\mathrm{MAX}}},$$

where d is the dimensionality of the system and $n_2(\mathbf{r})|_{\mathrm{MAX}}$ is the maximum value of $n_2(\mathbf{r})$ anywhere. We establish that, for the current system, $\omega_{\mathrm{RES}} = 0.3697(2\pi c)/a$, $\kappa = 0.037$ and the quality factor is $Q = \omega_{\mathrm{RES}}/2\gamma = 730$. For definiteness, we take $\delta = 4.25$, so bistability should be easily observable. We plot the analytical prediction as the green curve in Fig. 2; the dashed portion of that curve is unstable and therefore physically unobservable.

To verify our analytical prediction, we perform numerical experiments (nonlinear finite-difference time-domain[6] simulations with perfectly matched layers boundary conditions) on this system. These simulations solve Maxwell equations for a nonlinear medium exactly, without approximations apart for the discretization. We model a two-dimensional system, which decreases numerical requirements on our simulations significantly compared with three-dimensional simulations. Nevertheless, it was shown recently[7] that one can find an equivalent three-dimensional system that will behave in qualitatively the same manner as the two-dimensional system; the quantitative differences will only be of a geometrical factor close to 1. As shown in Fig. 2, this device displays optical bistability, and our analytical model is a very good representation of the physical reality. Throughout all these simulations, the observed reflections back into ports 1 and 3 are always less than 1% of the incoming signal's power.

We can use the analytical model to predict the performance of the device in a real physical setting. According to Ref. 7, once this device is implemented in a PC with a complete three-dimensional bandgap, the extent of the third dimension of all the modes will be roughly $\lambda/3$. Let us assume that the Kerr coefficient of the material that we are using is $n_2 = 1.5 \times 10^{-17}$ m^2/W (a value achievable in many nearly instantaneous nonlinear materials, e.g., As_2Se_2). Assuming a device with $Q = 4000$ (which is still compatible with 10-Gbit/s signals), and carrier wavelength $\lambda_0 = 1.55$ μm, we obtain the result that the characteristic power of the device is $P_0 \approx 15$ mW, and the peak operating power needed to observe bistability is roughly 24 mW (c.f. the 5-mW telecommunication peak power levels). The peak nonlinearly induced $\delta n/n < 0.001$, which is compatible with using nearly instantaneous nonlinear materials.

Let us now examine how we would use such a device for optical isolation. One of the biggest obstacles in achieving large-scale optics integration today is the nonexistence of integrated optical isolators (active and nonlinear devices typically do not tolerate small reflections coming from other devices that they are integrated with). The most common approach involves breaking the time-reversal symmetry by use of magneto-optic materials; other approaches involve breaking backward–forward symmetry by use of nonlinear materials.[8,9] Unfortunately, none of these approaches satisfies all the requirements mentioned earlier, which are necessary for large-scale optics integration. The device shown in Fig. 1 can perform integrated-optics isolation for most applications of interest, e.g., where the strength of each logical (forward-propagating) signal in a particular waveguide is above the bistability threshold and the reflected (backward-propagating) signals are weak. An example of such an operation is shown in Fig. 1. A strong forward-propagating signal (operating at a high-transmission point of the bistability curve) is nearly perfectly transferred from port 1 to port 4. However, when a weak reflected signal (operating at a low-transmission point of the bistability curve) enters port 4 of the devices at a later time, it proceeds to port 3, where it can be discarded.

In real practical applications, one will typically be launching pulses rather than cw signals into the

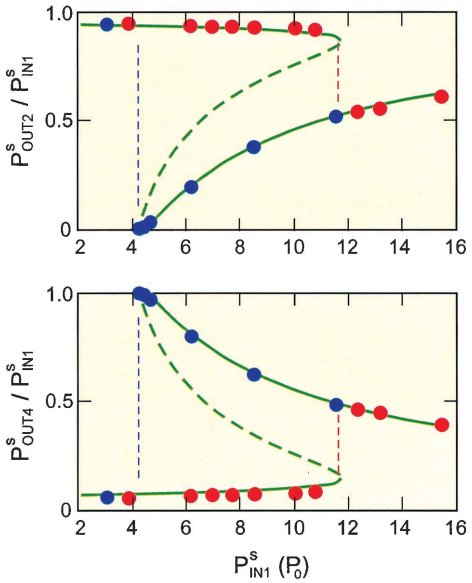

Fig. 2. Plots of the observed $T \equiv {P_{\mathrm{OUT}}}^S/{P_{\mathrm{IN}}}^S$ versus ${P_{\mathrm{IN}}}^S$ for the device from Fig. 1. Top, power observed at output 2; bottom, power observed at output 4. The input signal enters the device at port 1. To observe the lower bistability hysteresis branch (red circles), we send smooth cw signals into port 1 of the system, and we vary the peak power of the incoming signals. To observe the upper bistability hysteresis branch (blue circles), we launch superpositions of wide Gaussian pulses that decay into smaller-intensity cw signals, thereby relaxing into the points on the upper hysteresis branch. The green curves are from an analytical model described in the text.

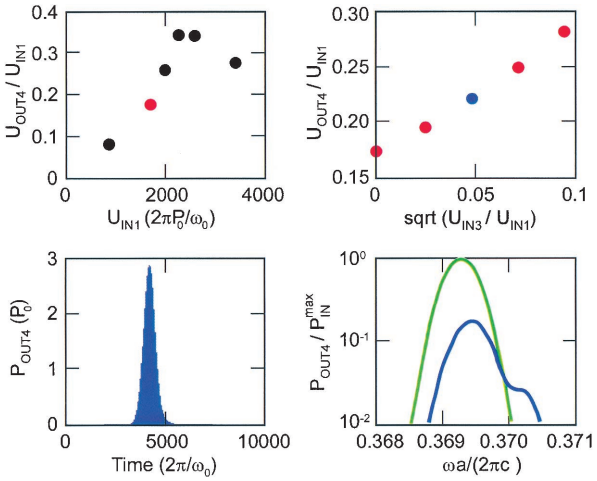

Fig. 3. Results of launching Gaussian pulses into the device of Fig. 1. Top left, observations of launching various energy (otherwise equal) pulses into port 1 only. Top right, observations of launching a fixed signal (red circle from the top left) into port 1 of the device, in parallel with launching various energy (otherwise equal) pulses into port 3. The blue shaded area and curve in the bottom graphs correspond to the pulse observed at port 4 when a signal (blue circle in the top right graph) is launched into the device. The top right graph also shows (in green) the incoming pulse (both pulses in this panel are normalized to the peak power of the incoming pulse).

device. Consequently, we also investigate what happens in this case. When the pulse duration is very long, the response is very similar to that of the cw case, following the red circles on the curve in Fig. 2. As the pulse duration decreases, we expect the features of this transmission curve to smooth out. To check this, we perform a series of numerical experiments in which we launch various-energy Gaussian pulses of carrier frequency $\omega_0 = \omega_{\mathrm{RES}} - 4.25\gamma$ and FWHM bandwidth $\omega_0/\mathrm{FWHM} = 638$ into port 1 of the device. The ratio of the energy transmitted to port 4 is shown at the top left of Fig. 3.

As an illustration of another possible application of our device, we now exploit this sharp on transition to construct an all-optical transistor. We perform a series of numerical experiments in which we launch into port 1 the pulses represented by the red circle in the top left panel of Fig. 3; however, in addition to this, we send identical (albeit smaller energy) pulses into port 3 of the system, as shown at the top right of Fig. 3. As one can see, the amplification can be quite drastic; for example, the pulse represented by the blue dot at the top right experienced an amplification factor of roughly 20. Such large amplifications are precisely the functionality that one expects from an all-optical transistor.[2] An additional interesting feature of the top right of Fig. 3 is that the energy observed at port 4 is essentially proportional to the square root of the energy sent in through port 3. This result means that the energy amplification factor becomes infinite as the signal energy goes to zero, which may have exciting new applications, for instance, for low threshold lasers. This behavior can be understood as follows: Pulses coming in through ports 1 and 3 are coherent and in phase. Consequently (taking into account the up–down symmetry of the system), once inside the cavities, the signals add in amplitude. Therefore, for small signals and a given pulse incoming through port 1, the energy stored in the cavity is a linear function of the field applied at port 3. Since the energy at port 4 is a linear function of the energy stored in the cavities, it is a linear function of the square root of the energy coming through port 3. If instead we considered a time-integrating nonlinearity, and temporally incoherent signals, for a fixed incoming pulse at port 1, the energy output at port 4 would be a linear function of the energy coming into port 3 (in that case, the signals in the cavity would add in intensity, rather than in amplitude). Finally, since the frequency width of the pulses is comparable with the frequency width of the cavity, and the nonlinear effects are quite extreme, it is important to determine possible distortions in the shapes of the output pulses. The use of finite-difference time-domain simulations provides a bonus here, since a detailed description of output pulses is typically not feasible with other theoretical models. In general, we find that the output pulses retain their pulse shape, as shown at the bottom of Fig. 3.

With only minor modifications, the device system that we have proposed can also be used for other applications,[1] including any all-optical logical gate, pulse reshaping and regeneration, noise cleanup, optical diodes,[3] and memory.

We thank Moti Segev from Technion, Israel, and Erich Ippen of the Massachusetts Institute of Technology for useful discussions. This work was supported in part by the Materials Research Science & Engineering Center program of the National Science Foundation under grant DMR-9400334. M. Soljačić's e-mail address is marin@alum.mit.edu.

References

1. B. E. A. Saleh and M. C. Teich, *Fundamentals of Photonics* (Wiley, New York, 1991).
2. M. Soljačić, M. Ibanescu, S. G. Johnson, Y. Fink, and J. D. Joannopoulos, Phys. Rev. E **66,** 055601(R) (2002).
3. S. F. Mingaleev and Y. S. Kivshar, J. Opt. Soc. Am. B **19,** 2241 (2002).
4. S. Fan, P. R. Villeneuve, J. D. Joannopoulos, and H. A. Haus, Phys. Rev. Lett. **80,** 960 (1998).
5. There also exist stable states of the system that are not left–right symmetric; we were able to excite them with particular initial conditions purposely designed to ruin the left–right symmetry. Nevertheless, the states that respect left–right symmetry appear to be particularly stable; various nonlinearly induced left–right asymmetries (at typcial operating power levels) with as large as 10% differences in the energies stored in the two cavities did not destabilize them.
6. For a review, see A. Taflove, *Computational Electrodynamics: The Finite-Difference Time-Domain Method* (Artech House, Norwood, Mass., 1995).
7. M. L. Povinelli, S. G. Johnson, S. Fan, and J. D. Joannopoulos, Phys. Rev. B **64,** 075313 (2001).
8. M. Scalora, J. P. Dowling, M. J. Bloemer, and C. M. Bowden, J. Appl. Phys. **76,** 2023 (1994).
9. K. Gallo, G. Assanto, K. R. Parameswaran, and M. M. Fejer, Appl. Phys. Lett. **79,** 314 (2001).